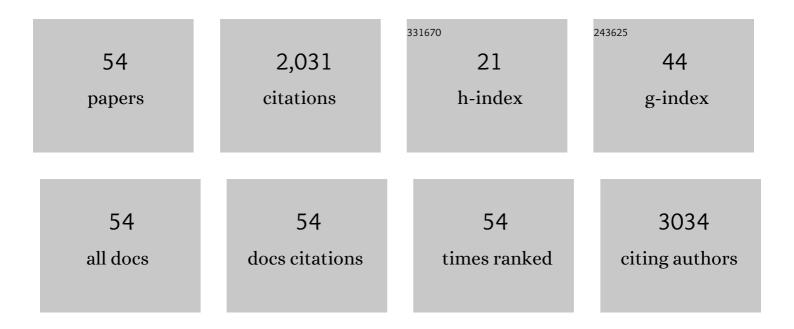
## Baofu Ding

List of Publications by Year in descending order

Source: https://exaly.com/author-pdf/788000/publications.pdf Version: 2024-02-01



#	Article	IF	CITATIONS
1	Dual Plasmonic Nanostructures for High Performance Inverted Organic Solar Cells. Advanced Materials, 2012, 24, 3046-3052.	21.0	654
2	Plasmonic Electrically Functionalized TiO <sub>2</sub> for Highâ€Performance Organic Solar Cells. Advanced Functional Materials, 2013, 23, 4255-4261.	14.9	138
3	Unsaturated Single Atoms on Monolayer Transition Metal Dichalcogenides for Ultrafast Hydrogen Evolution. ACS Nano, 2020, 14, 767-776.	14.6	106
4	Angstrom-confined catalytic water purification within Co-TiOx laminar membrane nanochannels. Nature Communications, 2022, 13, .	12.8	97
5	Investigation of the behaviour of electronic resistive switching memory based on MoSe2-doped ultralong Se microwires. Applied Physics Letters, 2016, 109, .	3.3	86
6	Mesoporous MnCo 2 O 4.5 nanoneedle arrays electrode for high-performance asymmetric supercapacitor application. Chemical Engineering Journal, 2017, 315, 491-499.	12.7	83
7	High-efficiency inverted polymer solar cells controlled by the thickness of polyethylenimine ethoxylated (PEIE) interfacial layers. Physical Chemistry Chemical Physics, 2014, 16, 23792-23799.	2.8	56
8	Efficient perovskite solar cell fabricated in ambient air using one-step spin-coating. RSC Advances, 2016, 6, 43299-43303.	3.6	52
9	Quantum conductance in MoS2 quantum dots-based nonvolatile resistive memory device. Applied Physics Letters, 2017, 110, .	3.3	43
10	Small-molecular organic solar cells with C60/Al composite anode. Organic Electronics, 2007, 8, 445-449.	2.6	39
11	AÂ2D material–based transparent hydrogel with engineerable interference colours. Nature Communications, 2022, 13, 1212.	12.8	37
12	Mechanism for bipolar resistive switching memory behaviors of a self-assembled three-dimensional MoS2 microsphere composed active layer. Journal of Applied Physics, 2017, 121, .	2.5	34
13	Sustainable and high-performance Zn dual-ion batteries with a hydrogel-based water-in-salt electrolyte. Energy Storage Materials, 2022, 47, 187-194.	18.0	33
14	PEIE capped ZnO as cathode buffer layer with enhanced charge transfer ability for high efficiency polymer solar cells. Synthetic Metals, 2015, 203, 243-248.	3.9	31
15	Synergetic Effect of Three-Dimensional Co 3 O 4 @Co(OH) 2 Hybrid Nanostructure for Electrochemical Energy Storage. Electrochimica Acta, 2016, 215, 298-304.	5.2	31
16	Highâ€Fidelity Transfer of 2D Bi <sub>2</sub> O <sub>2</sub> Se and Its Mechanical Properties. Advanced Functional Materials, 2020, 30, 2004960.	14.9	31
17	LiF Layer at the Interface of Au Cathode in Organic Light-Emitting Devices: A Nonchemical Induced Carrier Injection Enhancement. Journal of Physical Chemistry C, 2012, 116, 2543-2547.	3.1	30
18	Magnetoâ€optic effect of twoâ€dimensional materials and related applications. Nano Select, 2020, 1, 298-310.	3.7	30

Baofu Ding

#	Article	IF	CITATIONS
19	Giant magneto-birefringence effect and tuneable colouration of 2D crystal suspensions. Nature Communications, 2020, 11, 3725.	12.8	28
20	2D Functional Minerals as Sustainable Materials for Magnetoâ€Optics. Advanced Materials, 2022, 34, e2110464.	21.0	26
21	Viscous Solvent-Assisted Planetary Ball Milling for the Scalable Production of Large Ultrathin Two-Dimensional Materials. ACS Nano, 2022, 16, 10179-10187.	14.6	26
22	Delayed-switch-on effect in metal-insulator-metal organic memories. Applied Physics Letters, 2007, 91, 143511.	3.3	25
23	A Scalable Artificial Neuron Based on Ultrathin Two-Dimensional Titanium Oxide. ACS Nano, 2021, 15, 15123-15131.	14.6	25
24	Catalystâ€Free Growth of Atomically Thin Bi <sub>2</sub> O <sub>2</sub> Se Nanoribbons for Highâ€Performance Electronics and Optoelectronics. Advanced Functional Materials, 2021, 31, 2101170.	14.9	23
25	Simple in-situ growth of layered Ni 3 S 2 thin film electrode for the development of high-performance supercapacitors. Applied Surface Science, 2017, 399, 432-439.	6.1	21
26	Magnetic field modulated exciton generation in organic semiconductors: An intermolecular quantum correlated effect. Physical Review B, 2010, 82, .	3.2	20
27	A combined theoretical and experimental investigation on the transient photovoltage in organic photovoltaic cells. Applied Physics Letters, 2010, 96, .	3.3	16
28	Manipulating Electrocatalysis using Mosaic Catalysts. Small Science, 2021, 1, 2000059.	9.9	15
29	Crystallization process of perovskite modified by adding lead acetate in precursor solution for better morphology and higher device efficiency. Organic Electronics, 2017, 43, 189-195.	2.6	14
30	Using Magneto-Electroluminescence As a Fingerprint to Identify the Carrier-to-Photon Conversion Process in Dye-Doped OLEDs. Journal of Physical Chemistry C, 2011, 115, 20295-20300.	3.1	13
31	High-Contrast Tandem Organic Light-Emitting Devices Employing Semitransparent Intermediate Layers of LiF/Al/C <sub>60</sub> . Journal of Physical Chemistry C, 2012, 116, 24690-24694.	3.1	13
32	A cost-effective, long-lifetime efficient organic luminescent solar concentrator. Journal of Applied Physics, 2015, 118, 015502.	2.5	12
33	Collective Behavior Induced Highly Sensitive Magneto-Optic Effect in 2D Inorganic Liquid Crystals. Journal of the American Chemical Society, 2021, 143, 12886-12893.	13.7	12
34	Buffer-enhanced electron injection in organic light-emitting devices with copper cathode. Organic Electronics, 2013, 14, 511-515.	2.6	11
35	High contrast tandem organic light emitting devices. Applied Physics Letters, 2012, 101, 133305.	3.3	10
36	Modification of the organic/La0.7Sr0.3MnO3 interface by in situ gas treatment. Applied Surface Science, 2007, 253, 9081-9084.	6.1	9

BAOFU DING

#	Article	IF	CITATIONS
37	Loss and recovery of bistability of organic bistable devices. Organic Electronics, 2009, 10, 965-969.	2.6	9
38	Determination of capacitance-voltage characteristics of organic semiconductor devices by combined current-voltage and voltage decay measurements. Science China Technological Sciences, 2011, 54, 826-829.	4.0	9
39	Impact of alkyl chain length of 1,n-diiodoalkanes on PC71BM distribution in both bulk and air surface of PTB7:PC71BM film. Organic Electronics, 2016, 37, 358-365.	2.6	9
40	Impact of additive residue on the photodegradation of high performance polymer solar cells. Organic Electronics, 2017, 49, 226-233.	2.6	9
41	Encapsulation of Tandem Organic Luminescence Solar Concentrator With Optically Transparent Triple Layers of SiO <sub>2</sub> /Epoxy/SiO <sub>2</sub> . IEEE Journal of Selected Topics in Quantum Electronics, 2016, 22, 82-87.	2.9	8
42	Tuning Magneto-photocurrent between Positive and Negative Polarities in Perovskite Solar Cells. Journal of Physical Chemistry C, 2017, 121, 9537-9542.	3.1	8
43	Highly crystalline CsPbI <sub>2</sub> Br films for efficient perovskite solar cells <i>via</i> compositional engineering. RSC Advances, 2019, 9, 30534-30540.	3.6	7
44	Largely Tunable Magneto-Coloration of Monolayer 2D Materials via Size Tailoring. ACS Nano, 2021, 15, 9445-9452.	14.6	7
45	Photoemission study of C60-induced barrier reduction for hole injection at N, N′-bis(naphthalene-1-y1)-N, N′-bis(phenyl) benzidine/Al. Journal of Applied Physics, 2009, 105, 106105.	2.5	6
46	Room-temperature spin-polarized organic light-emitting diodes with a single ferromagnetic electrode. Applied Physics Letters, 2014, 104, .	3.3	5
47	A simple and cost effective experimental method for verifying singlet fission in pentacene–C <sub>60</sub> solar cells. RSC Advances, 2015, 5, 29718-29722.	3.6	5
48	A reduced electron-extraction barrier at an interface between a polymer poly(3-hexylthiophene) layer and an indium tin oxide layer. Organic Electronics, 2013, 14, 457-463.	2.6	4
49	Independent thickness and lateral size sorting of two-dimensional materials. Science China Materials, 2021, 64, 2739-2746.	6.3	4
50	Charge dynamics in solar cells with a blend of π-conjugated polymer-fullerene studied by transient photo-generated voltage. Physical Chemistry Chemical Physics, 2012, 14, 8397.	2.8	3
51	Simultaneous monitoring of singlet and triplet exciton variations in solid organic semiconductors driven by an external static magnetic field. Applied Physics Letters, 2014, 105, 013304.	3.3	3
52	Evidences of photocurrent generation by hole–exciton interaction at organic semiconductor interfaces. Organic Electronics, 2015, 26, 75-80.	2.6	3
53	A simple method to experimentally determine the accurate RC-constant in nanosecond timescale transient photocurrent measurements on organic solar cells. RSC Advances, 2015, 5, 103403-103409.	3.6	2
54	The effect of an external electric field on thermally-deposited thin CdS/CdTe-based solar cells. International Journal of Modern Physics B, 2015, 29, 1550238.	2.0	0